CHEMISTRY OF MATERIALS

Article

pubs.acs.org/cm

PEG-Graft Density Controls Polymeric Nanoparticle Micelle Stability

Jennifer Logie,[†,‡] Shawn C. Owen,[†,‡] Christopher K. McLaughlin,[†] and Molly S. Shoichet*[,†,‡,§]

[†]Department of Chemical Engineering and Applied Chemistry, [‡]Institute of Biomaterials and Biomedical Engineering, and the [§]Department of Chemistry, The Donnelly Centre, University of Toronto, Room 514, 160 College Street, Toronto, Ontario M5S 3E1, Canada

Supporting Information

ABSTRACT: Polymeric nanoparticle micelles typically comprise amphiphilic block copolymers, having a hydrophobic core that is useful for chemotherapeutic encapsulation, and a hydrophilic corona for aqueous stability. Formulations often require the use of excipients to overcome poor particle stability, yet these excipients can be cytotoxic. In order to create a stable polymeric nanoparticle micelle without the use of excipients, we investigate a series of amphiphilic polymers where the hydrophobic core composition and molar mass is maintained and the hydrophilic corona is varied. With the graft copolymer, poly(D,L-lactide-*co*-2-methyl-2-carboxy-trimethylenecarbonate)-*g*-poly(ethylene glycol) (P(LA-*co*-TMCC)-*g*-PEG), we demonstrate how PEG density can be tuned to improve the stability of the resulting self-assembled micelle. Increased PEG density leads to micelles that resist aggregation during lyophilization, allowing resuspension in aqueous media with narrow distribution. Furthermore, high PEG density micelles resist dissociation in serum protein containing media, with almost no dissociation seen in serum after 72 h. By changing the number of PEG chains per polymer backbone from 0.5 to 6, we observe increased stability of the nanoparticle micelles. All formulations are cytocompatible, as measured with MDA-MB-231 cells, and show no evidence for hemolysis, as measured with red blood cells. Importantly, PEG density does not impact drug loading within the nanoparticle micelle core, as demonstrated with the potent chemotherapeutic drug, docetaxel, confirming the role of the hydrophobic core for encapsulation. The surface properties of the polymeric nanoparticle micelles can thus be selectively modulated by variation in PEG density, which in turn influences stability, obviates the need for excipients and provides key insights into the design of drug delivery platforms.

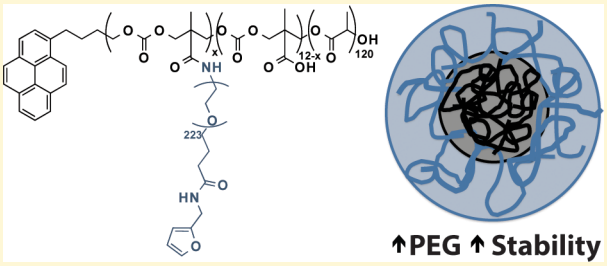

INTRODUCTION

Polymeric nanoparticle micelles have garnered significant attention over the past 20 years for targeted delivery of potent chemotherapeutics in cancer. Amphiphilic copolymers self-assemble in aqueous solution to have a hydrophobic core, in which hydrophobic small molecule drugs are encapsulated, and a hydrophilic corona, which provides stability in aqueous solutions. Given that chemotherapeutics are normally administered in dose-limiting organic solvents and surfactants, polymeric micelles provide a safer alternative for drug delivery by allowing increased dosing levels, prolonged systemic circulation, and greater tumor accumulation through the enhanced permeability and retention (EPR) effect.[1,2] Ideally, micelles are monodisperse, <200 nm in diameter, and stable to dilution in the presence of proteins.[3,4] Notwithstanding the many polymeric micelle formulations that have been studied, many have poor stability both *in vitro* and *in vivo*.[1,2,5,6]

The most common polymers used in nanoparticle micelles comprise a biocompatible hydrophobic block (e.g., poly(lactic acid), poly(caprolactone), poly(aspartic acid), poly(lactic-*co*-glycolic acid)) and a biocompatible hydrophilic block, usually poly(ethylene glycol) (PEG).[7−9] For decades PEG has been the polymer of choice for a variety of biomedical applications.[10,11] It is used clinically in a number of protein formulations to prevent premature clearance by the mononuclear phagocyte system and has been shown to be bioresorbable.[12−14] Several studies have also demonstrated limited protein adsorption and opsonization of PEG-modified nanoparticles - especially those used in solid particle platforms.[15−21] We designed a novel, biocompatible graft polymer of poly(D,L-lactide-*co*-2-methyl-2-carboxytrimethylene carbonate)-*g*-poly(ethylene glycol) (P(LA-*co*-TMCC)-*g*-PEG) that self-assembles into micelles in aqueous solution.[22,23] The graft polymer design exhibits a low critical micelle concentration (CMC) and can be easily modified with functional groups for conjugation of targeting antibodies and peptides by click chemistry, thereby enabling receptor-mediated endocytosis.[22,24,25]

Polymeric micelle stability is of critical importance during storage, handling and clinical use. Insight into thermodynamic stability can be gained by investigating the CMC and freeze-drying, while insight into kinetic stability can be tested with dynamic studies. Many polymeric micelle formulations are unstable under freeze-drying conditions, requiring the addition of excipients. For example, excipients can prevent nanoparticle fusion by interparticle bridging during the freeze-drying

Received: February 6, 2014
Revised: April 11, 2014
Published: April 14, 2014

process, yet can themselves be toxic, dose-limiting and thus ultimately undesirable.[26−29] To avoid the use of excipients, polymeric micelle formulations are prepared immediately prior to use or stored in aqueous solutions, but this is impractical and limits dosing. Despite the importance of polymeric micelle stability in circulation and the wide use of PEG in amphiphilic copolymers, it is surprising that there are few studies that investigate the effect of PEG density on lyophilization and serum stability of micelles.[15,16,19,30]

Polymeric micelles used clinically must remain stable after intravenous (IV) injection in order to be useful for targeted delivery. Upon IV injection, micelles are subject to a number of environmental changes including changes in salt concentration, significant dilution and contact with serum proteins. The CMC, the fundamental parameter of thermodynamic stability, is largely influenced by hydrophobic interactions of the amphiphilic polymer.[31] Polymeric micelles often have CMCs in the micromolar concentration range, yet these are often measured in water, which does not accurately reflect the complexity of serum. Polymeric micelles with lower CMCs are more stable with respect to dilution; however, CMC does not always accurately reflect how quickly the micelles will dissociate under environmental influences. The kinetic stability of a micelle reflects its behavior over time and during disassembly - a property that dramatically shifts with environmental changes. Micelle kinetic stability has been measured under physiological conditions by methods including FRET and conjugation of fluorogenic probes in the presence of serum proteins.[30,32−35] Although these experiments provide valuable insight into the rate of degradation of the micelles, the external probe itself may change the apparent stability of the formulation. Hammond and co-workers recently reported a probe-free strategy to assess the inherent kinetic stability of micelles in the presence of serum using size exclusion chromatography.[1,2,36]

Herein, we describe a newly designed amphiphilic polymeric nanoparticle micelle with both high thermodynamic and kinetic stability. Our P(LA-*co*-TMCC)-*g*-PEG polymers are composed of a gradient backbone of lactide and 2-methyl-2-carboxytrimethylene carbonate (composed of 90% LA and 10% TMCC) and grafted PEG chains (grafting is controlled to between 5 and 50% of TMCC backbone repeat units). With control of the graft chemistry, the number of PEG chains conjugated to the hydrophobic backbone is tuned, thereby providing a platform with which to investigate the role of PEG density on micelle stability. Using PEG of molar mass 10 kg/mol, we synthesized amphiphilic polymers having an average of 0.5−6 PEG chains per backbone, the molar mass of which is 12 kg/mol. We demonstrate the benefits of increased PEG density on the long-term storage and handling of micelles and under physiologically relevant conditions. These self-assembled polymeric micelles have a narrow size distribution, similar to other block copolymer amphiphilic polymeric micelles, yet have the advantage of allowing the number of PEG chains along the polymer backbone to be easily varied.[32,37−40] This approach provides key insights into design elements of other polymeric nanoparticle micelles. As proof of concept for use in drug delivery, we demonstrate the capacity of these polymeric micelles to encapsulate docetaxel, a potent chemotherapeutic anticancer drug with poor water solubility.

■ MATERIALS AND METHODS

Materials. All solvents and reagents were purchased from Sigma-Aldrich and used as received unless otherwise noted. Synthesis of 5-methyl-5-benzyloxycarbonyl-1,3-trimethylene carbonate (TMCC-Bn) was carried out as previously reported.[3,4,41] 3,6-dimethyl-1,4-dioxane-2,5-dione (Sigma-Aldrich, St. Louis, MO) and 1-[3,5-bis-(trifluoromethyl)phenyl]—3-[(1*R*,2*R*)-(−)-2(dimethylamino)-cyclohexyl] thiourea (Strem Chemicals, Newburyport, MA) were used as received in the synthesis of P(LA-*co*-TMCC). Boc-NH-PEG(10K)-NHS (Rapp Polymere, Tubingen, Germany) was modified according to previously published protocols.[1,2,5,6,41]

Instruments. ^{1}H NMRs were recorded at 400 MHz at room temperature using a Varian Mercury 400 spectrometer. The chemical shifts (δ) are in ppm. Molecular weights and polydispersity of P(LA-*co*-TMCC) were measured by gel permeation chromatography (GPC) in THF (containing 0.25% tetrabutyl ammonium bromide) relative to polystyrene standards at room temperature on a Waters 515 HPLC pump with a RI detector (VE3580) and a UV detector (KNAUER 2500) at a flow rate of 0.6 mL/min. Fluorescence and absorbance measurements were performed with the Tecan Infinite M200 Pro fluorescent plate reader. Serum stability studies were performed using a GE ÄKTA Purifier 10 Fast Protein Liquid Chromatography System equipped with a UV900 monitor. Docetaxel quantification was determined using an Agilent 1100 HPLC equipped with an AB Sciex API 4000 triple quadropole mass spectrometer with electrospray ionization source detector.

Synthesis of poly(D,L-lactide-*co*-2-methyl-2-carboxytrimethylene carbonate)-*g*-poly(ethylene glycol)-furan. P(LA-*co*-TMCC) was synthesized as previously described.[23] The copolymer (100 mg) was dissolved in DMF (5 mL). *N*,*N*′-diisopropylcarbodiimide (DIC, 100 uL) and hydroxybenzotriazole (HOBt, 16.88 mg) were added and the solution was stirred for 30 min at room temperature. NH_2−PEG-furan (10 kg/mol) was dissolved in 5 mL of DMF and added to the copolymer solution under argon. Varying equivalents (3−12) of PEG to backbone polymer were used to achieve the different graft densities. The reaction was stirred at room temperature for 24 h, after which 500 uL of borate buffer (pH 9, 500 mM) was added and the solution was dialyzed against distilled water. Unreacted PEG was removed using a Sepharose CL-4B column equilibrated with distilled water. Collected fractions with polymer were combined and lyophilized to give a white solid (∼60% yield). ^{1}H NMR ($CDCl_3$): δ1.23 (m, CH_3 from TMCC), 1.57 (m, CH_3 from LA), 3.64 (bs, PEG), 4.34 (m, methylene from TMCC), and 5.16 (m, CH from LA).

Micelle Preparation. Micelles were prepared by self-assembly in water as previously described.[23] P(LA-*co*-TMCC)-*g*-PEG (4 mg) was dissolved in DMF (1 mL). 50 uL of borate buffer (pH 9, 500 mM) was added and the solution was left at room temperature for 15 min. 0.5 mL of distilled water was added dropwise at a rate of ∼1 drop per 3 s. The solution was dialyzed against distilled water for 24 h, changing the water six times (dialysis membrane: MWCO of 2 kg/mol).

Lyophilization. Polymeric micelles (1.2 mg/mL in water) were prepared and flash frozen in liquid nitrogen with and without the addition of pluronic-F68 (P68) at 0.2 w/w polymer/excipient prior to lyophilization. After freeze-drying, formulations were resuspended in water to their original concentration and characterized by DLS.

Dynamic Light Scattering (DLS) and Zeta Potential. The hydrodynamic diameter and zeta potential of micelles was determined using a Malvern Zetasizer Nano ZS, equipped with a 4 mW, 633 nm laser. All samples were prepared at a concentration of 1 mg/mL and filtered through a NY-0.45 μm filter (Progene, QC, Canada) prior to use. Measurements were carried out at 25 °C. Hydrodynamic diameter was measured in polystyrene cuvettes (Küvetten, Germany). Hydrodynamic diameters (d_h) were calculated from the Stokes−Einstein equation $d_h = k_B T/3\pi\eta D$, where k_B is the Boltzmann constant, T is the absolute temperature, η is the solvent viscosity and D is the diffusion coefficient. The autocorrelation functions of the scattered intensity were analyzed by means of the cumulant method to yield the effective diffusion coefficient (D) as a function of the scattered angle. The average of 3−5 individual samples with 36 runs each is reported. Zeta potential was measured using folded capillary cells (Malvern, DTS 1060). The average of three individual samples, prepared under the same conditions with 36 runs each is reported.

Scheme 1. Synthesis of P(LA-*co*-TMCC)-*g*-PEG Followed by Preparation of Polymeric Micelles by Dialysis[a]

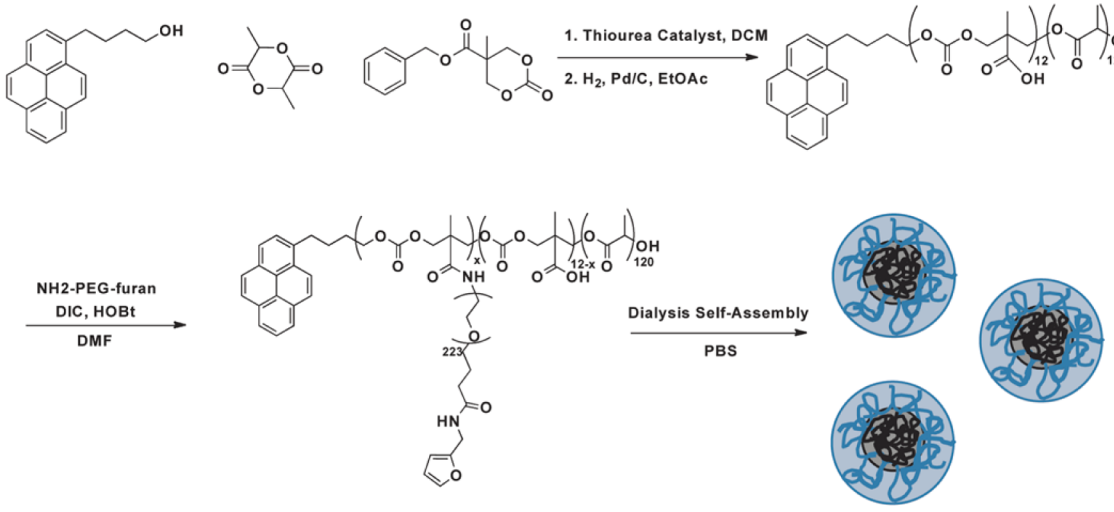

[a]The co-polymer backbone is synthesized by a ring-opening polymerization of the monomers D,L-lactide and 5-methyl-5-benzyloxycarbonyl-1,3-trimethylene carbonate (TMCC-Bn) initiated by 1-pyrenebutanol and catalyzed by a bifunctional thiourea. Following benzyl deprotection by palladium-catalyzed hydrogenolysis, bifunctional furan-poly(ethylene glycol)-amine (NH_2–PEG-furan) is grafted onto P(LA-*co*-TMCC) using diisopropylcarbodiimide (DIC) and hydroxybenzotriazole (HOBt) coupling chemistry. The resulting polymer is 90 mol % LA and 10 mol % TMCC, up to half of which have PEG grafted thereon. Micelles were formed by a dialysis self-assembly procedure against phosphate buffered saline (1×, PBS).

Transmission Electron Microscopy (TEM). TEM images were obtained with a Hitachi H-7000 conventional transmission electron microscope operated at 75 kV. Samples were prepared by placing three drops of particle solution at a concentration of 1 mg/mL in distilled water on a 400 mesh ultrathin carbon film on holey carbon support film copper grid (Ted Pella, Redding, CA). No heavy metal staining agents were used in grid preparation. The water was allowed to evaporate at room temperature prior to imaging. Particles were sized using ImageJ software, with sizes being an average of three individual batches, prepared under the same conditions with 10 particle measurements each.

CMC Measurement. Critical micelle concentrations of polymers in PBS (1×, pH 7.4) were determined using the standard pyrene procedure.[42] Briefly, 100 μL of pyrene solution (2 μg/mL in acetone) was added into glass vials. Acetone was allowed to evaporate overnight to form a pyrene film. 1 mL of polymer solution (from 0.1 μg/mL to 250 μg/mL in 1× PBS) was added into each vial and incubated for 24 h at room temperature while shaking. The fluorescence intensity was measured (excitation at 340 nm, emission 390 nm) as a function of polymer concentration. Micellization causes an abrupt change in quantum yield as the pyrene partitions into the hydrophobic core of micelles and its fluorescence intensity shifts.

Polymer Hemolysis and Cytotoxicity Assays. Hemolysis assays were performed following Hoffman's standard procedure.[43] Briefly, blood was collected from a human donor in 4 mL vacutainers coated with EDTA (BD Biosciences, Mississauga, ON). Serum was removed by centrifugation at 1500 rpm for 10 min. The whole blood was washed with 150 mM NaCl three times. After removing NaCl, the sample was increased to its original sample volume with 100 mM phosphate buffer at pH 7.4. The red blood cell solution was diluted 10× with phosphate buffer to give a suspension of 5×10^8 RBC/mL and used immediately. Micelle solutions were diluted with phosphate buffer to a total volume of 800 μL and mixed with 200 μL RBC solution to achieve final polymer concentrations of 1000, 800, 500, 250, 130, 65, and 33 μg/mL. After incubation for 1 h at 37 °C with mixing, solutions were centrifuged for 5 min at 5000 rpm. The supernatant was collected and the absorbance of lysed, oxygen-saturated hemoglobin was measured at 541 nm. For negative controls, red blood cells were incubated with 800 μL of phosphate buffer (PB, 100 mM) or 0.5 mg/mL dextran (60 kDa) to ensure that the polymeric material did not affect membrane integrity. For positive controls, red blood cells were incubated with deionized water or 1% Triton X-100, both of which are known to rupture membranes. The percent hemolysis was calculated according to the following equation:

$$\%\text{hemolysis} = \frac{\text{Abs(sample)} - \text{Abs(blank PB)}}{\text{Abs(positive control)} - \text{Abs(negative control)}} \times 100$$

For cytotoxicity assays, polymeric micelles (at 50 μg/mL polymer concentration) were incubated for 5 h with MDA-MB-231 cells seeded overnight in 96 well plates at a density of 1×10^3 cells/well in serum containing media. MDA-MB-231 were maintained (<8 passages) in RPMI 1640 growth medium supplemented with 10% FBS, 10 μg/mL penicillin and 10 μg/mL streptomycin. Lactate dehydrogenase assays were performed following the Roche procedure to determine cytotoxicity of polymers (Roche Applied Science, Laval, QC). The cytotoxicity was calculated relative to a positive control (2% Triton-X) and a negative control (cells alone) based on the absorbance of the samples at 490 nm. The experiment was repeated three times, with four wells per experiment for each polymer formulation.

$$\%\text{cytotoxicity} = \frac{\text{experimental value} - \text{negative control}}{\text{positive control} - \text{negative control}} \times 100$$

Serum Stability. Stability was assessed using Fast Protein Liquid Chromatography in a method adapted from Hammond et al.[36] Samples were run through a Superdex 200 gel filtration column with a flow rate of 1 mL/min and 1× PBS (pH 7.4) as the mobile phase. Micelles at a concentration of 1 mg/mL in 1× PBS were incubated with 20% fetal bovine serum (FBS, HyClone, Thermo Scientific). At specific time points after incubation with serum (0, 6, 24, 48, and 72 h), 500 μL aliquots were removed and injected onto the column. Elution peak areas were calculated using UNICORN software version 5.31.

Docetaxel Loaded Micelles. Docetaxel (DTX) loaded micelles were prepared using the same micellization procedure as described above for polymer alone, except with the addition of 2.4 mg of DTX to the dissolved polymer solution. Free DTX, which is insoluble in water and forms large aggregates, was removed by filtration through a 0.45 μm nylon filter. To determine drug loading, 10 μL of DTX-loaded micelles were diluted 1000× into a 50:50 mixture of acetonitrile and water and analyzed by high performance liquid chromatography coupled with tandem mass spectrometry (HPLC-MS/MS). The drug

dx.doi.org/10.1021/cm500448x | *Chem. Mater.* 2014, 26, 2847−2855

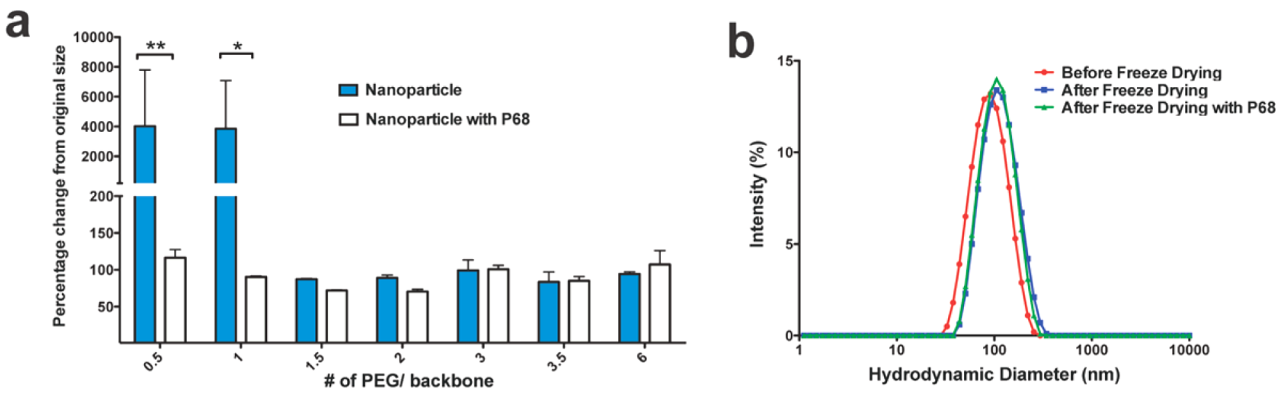

Figure 1. Effect of PEG density on nanoparticle micelle stability after lyophilization. (a) As measured by dynamic light scattering, the percent change in diameter of polymeric nanoparticle micelles upon reconstitution in aqueous solution after freeze-drying with or without the excipient Pluronic-F68 (P68) (n = 3, mean ± standard deviation, ** $p < 0.05$, * $p < 0.01$ determined by one way ANOVA and Bonferroni posthoc test). (b) Size distribution of high PEG (6 PEG/backbone) density nanoparticle micelles: before freeze-drying, after freeze-drying with the excipient P68 and after freeze-drying without excipients.

Table 1. Characterization of Low (1 PEG/backbone, bb), Medium (3.5 PEG/bb), and High (6 PEG/bb) PEG Density Polymers and Micelles

PEG density	PEG/bb[a]	M_n (kg/mol)[a]	CMC (μM)[b]	N_{agg} ($\times 10^3$)[c]	micelle distribution[d]
low	1	22	0.54 ± 0.06	1.32	0.156
medium	3.5	47	0.55 ± 0.05	3.37	0.158
high	6	72	0.37 ± 0.04	5.98	0.093

[a]Average PEG number per backbone and total polymer molar mass were obtained by ^{1}H NMR. [b]CMC was measured by the pyrene method, n = 4, mean ± standard deviation. [c]N_{agg} is an estimate of the number of polymer chains aggregated in one micell.e [d]Distribution of micelles in PBS is determined by dynamic light scattering.

loading was quantified by comparing to a DTX standard curve (3.125−200 ng/mL) using paclitaxel as an internal standard (100 ng/mL).

Statistics. All statistical analyses were performed using Graph Pad Prism version 5.00 for Macintosh (Graph Pad Software, San Diego, California, www.graphpad.com). Differences among groups were assessed by one-way ANOVA with Bonferroni *post hoc* correction to identify statistical differences among three or more treatments. Alpha levels were set at 0.05 and a p-value of ≤0.05 was set as the criteria for statistical significance. Graphs are annotated where p-values are represented as $*p \leq 0.05$, $**p \leq 0.01$, or $***p \leq 0.001$. All data are presented as mean ± standard deviation.

RESULTS

Polymer Synthesis and Micellization. P(LA-*co*-TMCC) was synthesized by a ring-opening polymerization of D,L-lactide and benzyl protected TMCC (TMCC-Bn) using a pyrenebutanol initiator and a bifunctional thiourea catalyst, as shown in Scheme 1.[23]

The polymer backbone was characterized by GPC to have an M_n of 12 500 g/mol and a polydispersity index of 1.13 relative to polystyrene standards. ^{1}H NMR showed a composition of 10 mol % TMCC and 90 mol % LA by comparing the integration of peaks at 4.33 ppm (27) and 5.17 ppm (123), respectively. After deprotection of the benzyl group on TMCC, PEG was grafted onto the backbone using DIC and HOBt. The graft density was controlled by varying the molar equivalents of PEG to the hydrophobic backbone. PEG density was calculated by ^{1}H NMR (Supporting Information Figure S1) by comparing the proton peak associated with the ethylene oxide of PEG (δ 3.64 ppm) to that associated with the lactide of PLA (δ 5.17 ppm). By ^{1}H NMR, we observed no evidence of PLA backbone cleavage, demonstrating that NH_2−PEG reacted with activated TMCC esters, as expected. Seven batches of polymers were synthesized with densities ranging from 0.5 to 6 PEGs per backbone (representing between 30 and 80 wt % of the total polymer). A maximum density of 6 PEGs/backbone was obtained (representing 50% of the free carboxylic acids along the backbone), with maximum conjugation likely due to steric hindrance of the large molar mass PEG chains.

Micelles were formed by self-assembly whereby the water-insoluble P(LA-*co*-TMCC)-*g*-PEG is dissolved in DMF and dialyzed against water.[22,23] The process is likely entropically driven; water molecules bound to the hydrophobic P(LA-*co*-TMCC) backbone are freed as the backbone aggregates together to form the micelle core.[44] The hydrophilic PEG chains form the micelle corona, thereby stabilizing the hydrophobic−hydrophilic interface by limiting the interaction between the core and the aqueous solution.[44]

Micelle Lyophilization and Resuspension. Since excipients, such as P68, have been shown to protect micelles against aggregation through lyophilization,[45] we studied lyophilization of our polymeric particles with and without P68 as a function of PEG substitution. Micelles with low PEG densities (i.e., 0.5 or 1 PEG/backbone) form large polydisperse aggregates upon freeze-drying that cannot be disrupted by sonication to polymeric micelles upon resuspension in aqueous solutions. These low density PEG micelles require the addition of P68 for resuspension after lyophilization, as shown in Figure 1 and Figure S2 (Supporting Information). As the PEG density increases, the addition of P68 is unnecessary as freeze-dried micelles are resuspended to their original micelle size without evidence of aggregation. Micelles with docetaxel encapsulated showed an identical trend, as shown in Figure S3 (Supporting Information).

Micelle Optimization. In order to better assess the influence of PEG density on nanoparticle micelle stability,

dx.doi.org/10.1021/cm500448x | *Chem. Mater.* 2014, 26, 2847−2855

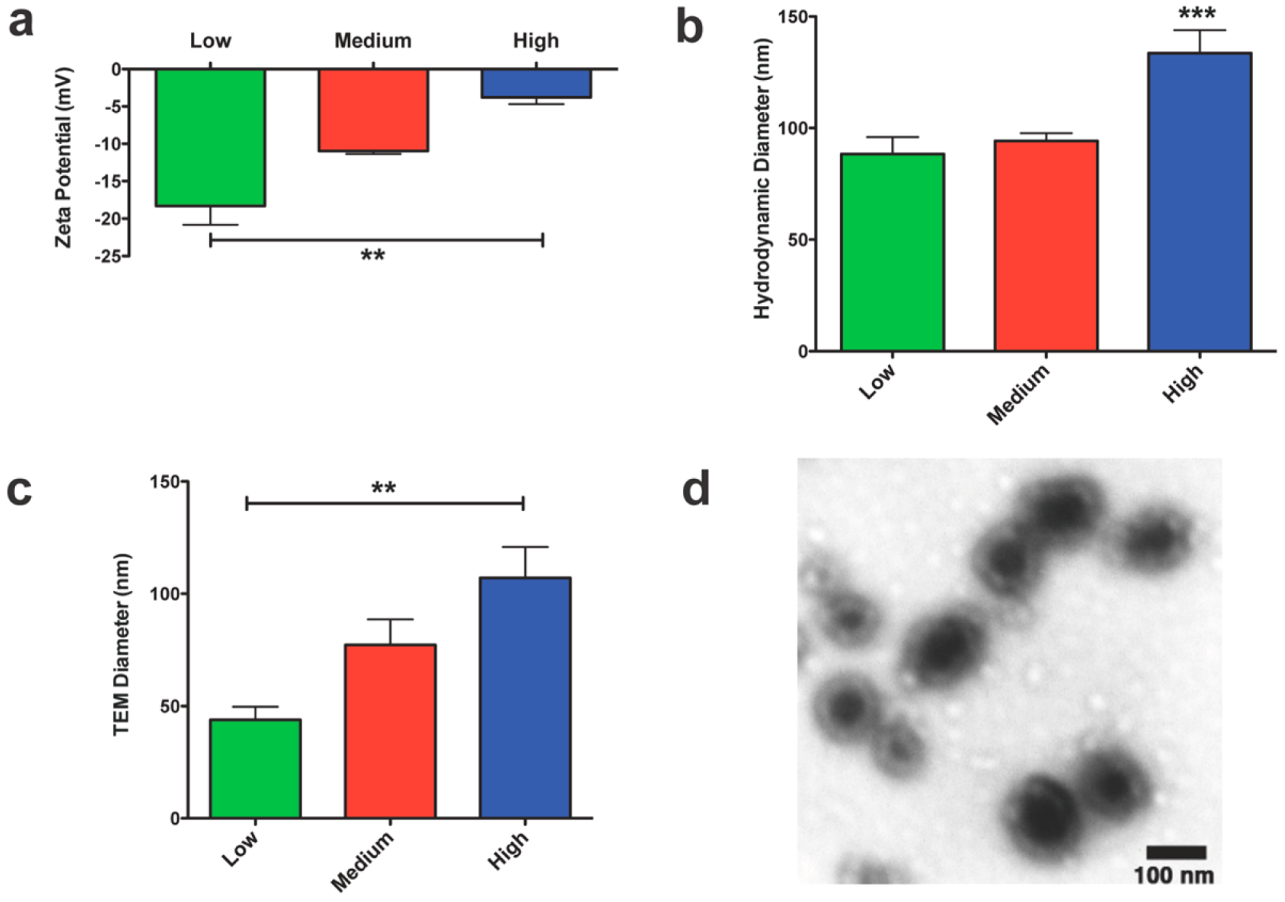

Figure 2. Micelle characterization. (a) Zeta potential measurements of micelles in water at 1 mg/mL: zeta potential increases toward neutral with increased PEG density. (b) Hydrodynamic diameter determined by DLS: polymeric nanoparticle micelle diameter increases at high PEG density. (c) Nanoparticle micelle diameter measured by TEM increases with increased PEG density. TEM diameters are less than DLS diameters because TEM measures the dry state whereas DLS measures the hydrated state. (d) Representative TEM image of high PEG density nanoparticle micelles clearly shows individual nanoparticle micelles (scale bar is 100 nm). No heavy metal staining agents were used in TEM image. Additional TEM image shown in Figure S5. For parts a, b, and c: $n = 3$ independent batches of micelles, mean + standard deviation, ** $p < 0.01$ and ***$p < 0.001$ by one-way ANOVA.

three micelle formulations were chosen for further characterization in terms of micelle diameter, micelle size distribution/polydispersity, and stability in protein rich aqueous solutions, as shown in Table 1: 1 PEG/backbone (low PEG density), 3.5 PEG/backbone (medium PEG density), and 6 PEG/backbone (high PEG density).

The CMCs of polymers, summarized in Table 1, were determined using the standard pyrene procedure as shown in Figure S4.[36,42] The CMCs of P(LA-*co*-TMCC)-*g*-PEG polymers ranged from 0.37 to 0.54 μM, with the high PEG density polymer having the lowest CMC. The trend in decreasing CMC and increasing aggregation number is attributed to the decrease in carboxylic acids within the core, making the core more hydrophobic and reducing repulsion between backbone polymer chains.[23]

The negative surface charge of polymeric micelles with low PEG density increased toward neutral with increased PEG density, as measured by zeta potential (Figure 2a). There are two contributing reasons for this phenomenon: (1) with increased PEG density there are fewer free TMCC carboxylate ions within the core that normally contribute to the negative surface potential and (2) with increased PEG density, the remaining TMCC carboxylates within the core are better shielded.

Size measurements by DLS and TEM showed an increase in diameter with an increase in PEG density (Figure 2b,c). TEM measurements were smaller than those by DLS, consistent with the dehydrated state of the micelles when they are measured using this technique. Notably, low PEG density micelles tended to aggregate during dehydration and form thin films making them difficult to image, an effect that was not seen when dehydrating high PEG density micelles. Even in areas of poor dispersion on the TEM grid, micelles of high PEG density polymers did not flocculate or form thin films (Figure 2d, S5). All polymeric micelles had diameters <150 nm, suggesting that they are suitable for studies that rely on the EPR effect.

Hemolysis and Cytocompatibility of Polymeric Micelles. P(LA-*co*-TMCC)-*g*-PEG micelles of low, medium and high PEG densities were evaluated for hemolysis with red blood cells and cytotoxicity with metastatic breast cancer MDA-MB-231 cells. Since common excipients to solubilize chemotherapeutics can cause undesirable side effects, we wanted to ensure that the nanoparticles micelles themselves are not cytotoxic and are good candidates for use as drug delivery vehicles. Micelles were incubated with human red blood cells to check for hemolysis. All three formulations showed no hemolysis, as quantified relative to the amount of heme released into pure water and detected by absorbance at 451 nm

dx.doi.org/10.1021/cm500448x | *Chem. Mater.* 2014, 26, 2847−2855

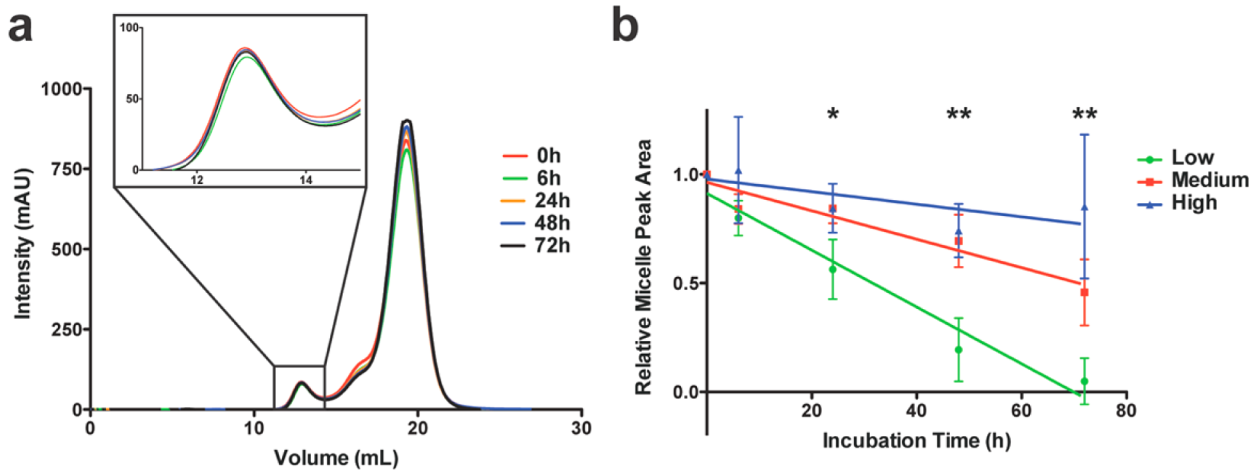

Figure 3. (a) SEC traces at 280 nm of high PEG density micelles incubated with 20 vol % FBS for different time periods at 37 °C show clear separation of the polymeric nanomicelles (eluent at 12 mL) from FBS proteins (eluent at 18 mL). (b) Change in peak area of micelles as a function of incubation time. Decrease in peak area indicates micelle dissociation: high PEG density micelles are the most stable, followed by medium and then low PEG density micelles (n = 4, mean ± standard deviation, * p < 0.05, ** p < 0.01 by one-way ANOVA followed by Bonferroni posthoc test).

(Figure S6). Cytotoxicity was assessed by the lactate dehydrogenase (LDH) assay after incubation of the micelles with MDA-MB-231 cells. All formulations showed no cytotoxicity relative to a positive control (2% Triton-X) and a negative control (untreated cells) (Supporting Information Figure S6). These data demonstrate that all three micelle formulations are cytocompatible.

Kinetic Stability. In order to assess the kinetic stability of micelles with varying PEG densities, micelles (1 mg/mL) were incubated in the presence of FBS (20 vol %) at 37 °C. 20% serum represents a good proxy for both in vitro and in vivo studies, while still allowing micelles to be separated and quantified by FPLC as a direct measure of their stability. At selected times, up to 72 h, the micelles were separated from serum proteins using size exclusion chromatography (SEC) on a Superdex 200 column. The micelle stability was associated with the peak intensity at 280 nm at 12 mL eluant: a decrease in peak area indicates micelle dissociation.

As shown in Figure 3a, the peak at 12 mL corresponds to the micelle peak, while the peak at 18 mL corresponds to the various serum proteins in FBS as well as dissociated, free polymer chains (Supporting Information Figure S7). The micelle formulations were compared by relative micelle peak area over time, as shown in Figure 3b. At high PEG density, the micelle peak did not change significantly as a function of time (p > 0.05), suggesting little micelle dissociation over the 72 h period. The low PEG density micelle peak area decreased significantly over time due to the dissociation of micelles in the presence of serum proteins, with no micelles detectable at 72 h. Linear regression analysis shows that the slopes representing the dissociation of the three PEG density formulations were significantly different (p < 0.002). Significant differences were detected between formulations at 24 (p < 0.05), 48, and 72 h (p < 0.01), while there was no significant difference at 6 h. Half-lives of the formulations (i.e., when 50% of the micelles are dissociated) were estimated by the time at which the micelle peak area had decreased to 50% of its initial value. The low PEG density micelles have a half-life of 32 ± 5 h and medium PEG density micelles have a half-life of 71 ± 12 h. A half-life for the high PEG density micelles could not be estimated over this time period, as the slope of the line for the decrease in peak area was not significantly different from zero.

DTX Loading. To understand whether these P(LA-*co*-TMCC)-*g*-PEG micelles would be effective drug delivery vehicles, the loading of a hydrophobic chemotherapeutic, docetaxel, was assessed using HPLC-MS/MS. There was no significant difference in terms of drug loading as a function of PEG density (Figure 4), suggesting that loading of this hydrophobic drug is dictated only by the hydrophobic interactions within the core. Since the core molar mass and chemical structure were not changed by PEG grafting density, the drug loading was constant for all formulations at approximately 10 wt % relative to the hydrophobic core; however, when compared to the total mass of the polymer micelle, percent loading necessarily decreases with increased PEG density (Supporting Information Figure S8).

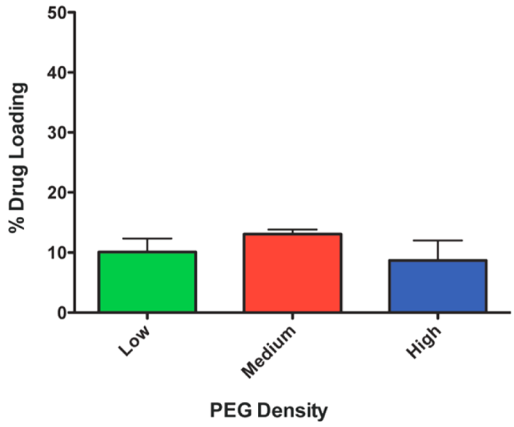

Figure 4. Percent drug loading relative to the mass of the hydrophobic backbone, P(LA-*co*-TMCC). The level of PEG density did not significantly affect the relative amount of drug loaded per micelle (n = 4, mean ± standard deviation, p = 0.15 by one-way ANOVA between all groups).

■ DISCUSSION

PEG is known to prevent protein adsorption and particle opsonization, and for this reason has been integrated into a

dx.doi.org/10.1021/cm500448x | *Chem. Mater.* 2014, 26, 2847−2855

variety of particle platforms intended for clinical use.[46,47] Despite the prevalence of PEG as the hydrophilic block in polymer micelles, there has been limited research on the effect of PEG density on nanoparticle micelle stability, which is critical to their ultimate success clinically. Several groups have shown the shielding effect associated with increased PEG molecular weight, but even with high molecular weight PEG, polymeric micelles often requires the use of excipients for stabilization.[16,26] Composition of the copolymer used here, P(LA-*co*-TMCC), provides a convenient platform to control the graft density of high molecular weight PEG. In addition, PEG grafting to TMCC carboxylic acid groups can be achieved throughout the backbone and is not limited to terminal polymer modification with higher molecular weight or branched PEGs, as is required by other systems.[16,48] This unique graft architecture allows us to control PEG conjugation along the polymer chain in order to produce brush-like polymer morphologies that self-assemble into well-defined nanoparticle micelles.

The ability to lyophilize micelles and resuspend them without aggregation enables dry product storage, eliminating concerns of solution stability of polymer, micelle, and drug. Numerous micelle formulations have had limited use due to the necessity for fresh preparation prior to use.[49] To overcome this, micelle syntheses often require the addition of excipients as stabilizers for the freeze-drying process, which increases both the complexity and potential cytotoxicity of the formulation. Common excipients used to stabilize nanoparticle micelles are known to cause a number of side effects such as rupturing cell membranes, hypersensitivity reactions, erythrocyte aggregation, and peripheral neuropathy.[27,50−52] Moreover, PEG-based micelles are particularly notorious for crystallizing during freeze-drying, causing significant aggregation even with the addition of polysaccharides.[53,54] Prud'homme and colleagues successfully lyophilized several different micelle formulations, including PLA-*co*-PEG, with the addition the P68.[29] In this study, we found that only the low PEG density P(LA-*co*-TMCC)-*g*-PEG micelles required P68 in order to prevent aggregation of particles during lyophilization. P68 is a block terpolymer of poly(ethylene oxide)-poly(propylene oxide)-poly(ethylene oxide), (PEO-PPO-PEO). Its proposed mechanism of stabilization is based on the PPO adsorbing onto the particle surface and the PEO intercalating between the nanoparticle micelle PEG chains, thereby causing the PEG chains to adopt a more extended conformation.[55] This extended brush-like conformation sterically stabilizes the particles.[56] Higher PEG densities incorporated into our polymeric micelles appear to have the same effect as this excipient, but without the added complexity and toxicity concerns associated with P68. The crowded surface prevents coalescence at high polymer concentrations during freeze-drying, critical for resuspension without changes in either size or polydispersity. This effect was confirmed by TEM where high PEG density micelles were easily imaged, even in areas of high polymer concentration on the grid, as they maintained their structure without aggregating into a film. In summary, the architecture of our copolymer facilitates the stabilization of micelles through both freeze-drying and concentrating procedures.

Interestingly, all PEG density formulations had CMCs between 0.37 and 0.54 μM, suggesting that they are thermodynamically stable. This is of particular interest considering the increase in hydrophilic PEG between formulations (from 30 to 80 wt %)—an effect which contrasts what is seen in linear systems, where it has been shown that an increase in the length of the hydrophilic block also increases the CMC.[44] Since all of our P(LA-*co*-TMCC)-*g*-PEG copolymers differ only in the number of PEG chains, the low CMCs of all formulations suggest that micelle thermodynamic stability is dictated not by the hydrophilic corona, but rather the length, hydrophobicity, and cohesion of the hydrophobic polymer within the core of our graft copolymers.[8,57] The CMCs of our polymers, measured using the standard pyrene method, are all lower than Pluronics and many common amphiphilic polymers, such as PLA−PEG diblock copolymers, indicating that they are less susceptible to disassembly upon dilution, which is key for administration by intravenous injection.[2]

Colloidal systems typically flocculate because they lack electrostatic repulsion at neutral zeta potential.[58] However, our polymeric nanoparticle micelles are stable as zeta potential increases to neutral, which is likely due to steric repulsion among the higher density of PEG chains that forces an extended brush-like conformation in the corona.[59] By reducing contact between micelles, the higher PEG density also may diminish van der Waals forces of attraction between the particles that usually account for their flocculation.[58] As negatively charged species are often cleared more rapidly than neutral species by immune cells,[60−62] we anticipate that our micelles will result in less opsonization and longer resident circulation times *in vivo*.

To test kinetic stability, we assessed the dissociation of micelles over time in the presence of serum containing cell culture media. The more physiological composition (protein, salt, pH, etc.) of this medium can shift the equilibrium between the free polymer chains and the micelle, resulting in more rapid dissociation. As expected, low PEG density micelles, while still having a half-life greater than 30 h, began dissociating almost immediately after incubation. In contrast, high PEG density micelles are more kinetically stable, with almost no dissociation over a 72 h incubation at 37 °C. The presence of proteins in the blood upon intravenous injection is well-known to destabilize micelles due to protein adsorption on the surface, so the improved kinetic stability of high PEG density micelles is likely beneficial for future in vivo studies.

While the kinetic and thermodynamic stability of the polymeric nanoparticle micelles are influenced by the hydrophilic corona, the loading of a hydrophobic drug is predominantly influenced by the hydrophobic block composition. Here, increasing the graft PEG density did not significantly change the drug loading of the potent chemotherapeutic docetaxel, which has a similar drug loading to that achieved with other polymeric micelles.[8,63,64] To further enhance drug loading, polymeric nanoparticle micelle core modifications may be investigated with this system.[39,65−67]

■ CONCLUSIONS

With our gradient copolymers of P(LA-*co*-TMCC)-*g*-PEG, we have demonstrated both near monodisperse synthesis and control over PEG graft density. Subsequent self-assembly into polymeric micelles allowed us to study the role of PEG graft density on both thermodynamic and kinetic stability. Although choosing an "optimal" PEG density will depend on many factors, here we show a unique graft polymer morphology that can be used to prepare polymeric micelles with desirable drug delivery properties (low CMC, kinetic and thermodynamic stability, minimal cytotoxicity). In future work, PEG can be

functionalized with targeting ligands to provide a strategy for either receptor-mediated endocytosis[1,68−70] or enhanced stealth evasion of the native immune system.[71,72] Overall, controlling unimer composition by tuning PEG graft density has clear implications for enhancing micelle stability and thus presents a strategy that can be broadly applied to other amphiphilic self-assembling polymeric systems intended for drug delivery applications.

■ ASSOCIATED CONTENT

Supporting Information

Additional figures as described in the text. This material is available free of charge via the Internet at http://pubs.acs.org.

■ AUTHOR INFORMATION

Notes

The authors declare no competing financial interest.

■ ACKNOWLEDGMENTS

We thank Professor Robert Prud'homme (Princeton University) for insight into lyophilization of polymeric micelles and Professor Mitchell Winnik and Peng Liu (both at the University of Toronto) for the use of their GPC. We are grateful for partial funding from the Natural Sciences and Engineering Research Council of Canada (MSS, PGSD to J.L. and PDF to C.K.M.) and the Canadian Institutes of Health Research (MSS).

■ REFERENCES

(1) Wang, A. Z.; Langer, R.; Farokhzad, O. C. *Annu. Rev. Med.* **2012**, *63*, 185−198.
(2) Kataoka, K.; Harada, A.; Nagasaki, Y. *Adv. Drug Deliver Rev.* **2012**, 1−20.
(3) Maeda, H.; Seymour, L. W.; Miyamoto, Y. *Bioconjugate Chem.* **1992**, *3*, 351−362.
(4) Davis, M. E.; Chen, Z. G.; Shin, D. M. *Nat. Rev. Drug Discovery* **2008**, *7*, 771−782.
(5) Duncan, R.; Gaspar, R. *Mol. Pharmaceutics* **2011**, *8*, 2101−2141.
(6) Elsabahy, M.; Wooley, K. L. *Chem. Soc. Rev.* **2012**, *41*, 2545−2561.
(7) Torchilin, V. P. *Cell. Mol. Life Sci.* **2004**, *61*, 2549−2559.
(8) Gaucher, G.; Dufresne, M.; Sant, V.; Kang, N.; Maysinger, D.; Leroux, J. *J. Controlled Release* **2005**, *109*, 169−188.
(9) Peer, D.; Karp, J. M.; Hong, S.; Farokhzad, O. C.; Margalit, R.; Langer, R. *Nat. Nanotechnol.* **2007**, *2*, 751−760.
(10) Abuchowski, A.; van Es, T.; Palczuk, N. C.; Davis, F. F. *J. Biol. Chem.* **1977**, *252*, 3578−3581.
(11) Park, K. *J. Controlled Release* **2010**, *142*, 147−148.
(12) Veronese, F. M.; Pasut, G. *Drug Discovery Today* **2005**, *10*, 1451−1458.
(13) Pasut, G.; Veronese, F. M. *Adv. Drug Deliver Rev.* **2009**, *61*, 1177−1188.
(14) Ryan, S. M.; Mantovani, G.; Wang, X.; Haddleton, D. M.; Brayden, D. J. *Expert Opin. Drug Delivery* **2008**, *5*, 371−383.
(15) Perry, J. L.; Reuter, K. G.; Kai, M. P.; Herlihy, K. P.; Jones, S. W.; Luft, J. C.; Napier, M.; Bear, J. E.; DeSimone, J. M. *Nano Lett.* **2012**, *12*, 5304−5310.
(16) Gref, R.; Lück, M.; Quellec, P.; Marchand, M.; Dellacherie, E.; Harnisch, S.; Blunk, T.; Müller, R. H. *Colloids Surf., B* **2000**, *18*, 301−313.
(17) Walkey, C. D.; Olsen, J. B.; Guo, H.; Emili, A.; Chan, W. C. W. *J. Am. Chem. Soc.* **2012**, *134*, 2139−2147.
(18) Gref, R.; Minamitake, Y.; Peracchia, M.; Trubetskoy, V.; Torchilin, V.; Langer, R. *Science* **1994**, *263*, 1600−1603.
(19) Aggarwal, P.; Hall, J. B.; McLeland, C. B.; Dobrovolskaia, M. A.; McNeil, S. E. *Adv. Drug Delivery Rev.* **2009**, *61*, 428−437.
(20) Kim, S. Y.; Zukoski, C. F. *Macromolecules* **2013**, *46*, 6624−6643.
(21) Kingshott, P.; Thissen, H.; Griesser, H. J. *Biomaterials* **2002**, *23*, 2043−2056.
(22) Shi, M.; Shoichet, M. S. *J. Biomater. Sci., Polym. Ed.* **2008**, *19*, 1143−1157.
(23) Lu, J.; Shoichet, M. S. *Macromolecules* **2010**, *43*, 4943−4953.
(24) Lu, J.; Shi, M.; Shoichet, M. S. *Bioconjugate Chem.* **2009**, *20*, 87−94.
(25) Chan, D. P. Y.; Owen, S. C.; Shoichet, M. S. *Bioconjugate Chem.* **2013**, *24*, 105−113.
(26) Layre, A. M.; Couvreur, P.; Richard, J.; Requier, D.; Ghermani, N. E.; Gref, R. *Drug Dev. Ind. Pharm.* **2006**, *32*, 839−846.
(27) Gelderblom, H.; Verweij, J.; Nooter, K.; Sparreboom, A. *Eur. J. Cancer* **2001**, *37*, 1590−1598.
(28) Tije, A. J. T.; Verweij, J.; Loos, W. J.; Sparreboom, A. *Clin. Pharmacokinet.* **2003**, *42*, 665−685.
(29) D'Addio, S. M.; Prud'homme, R. K. *Adv. Drug Delivery Rev.* **2011**, *63*, 417−426.
(30) Lu, J.; Owen, S. C.; Shoichet, M. S. *Macromolecules* **2011**, *44*, 6002−6008.
(31) Owen, S. C.; Chan, D. P. Y.; Shoichet, M. S. *Nano Today* **2012**, *7*, 53−65.
(32) Diezi, T. A.; Bae, Y.; Kwon, G. S. *Mol. Pharmaceutics* **2010**, *7*, 1355−1360.
(33) Chen, H.; Kim, S.; He, W.; Wang, H.; Low, P. S.; Park, K.; Cheng, J.-X. *Langmuir* **2008**, *24*, 5213−5217.
(34) Savić, R.; Azzam, T.; Eisenberg, A.; Maysinger, D. *Langmuir* **2006**, *22*, 3570−3578.
(35) Murakami, M.; Cabral, H.; Matsumoto, Y.; Wu, S.; Kano, M. R.; Yamori, T.; Nishiyama, N.; Kataoka, K. *Sci. Transl. Med.* **2011**, *3*, 64ra2−64ra2.
(36) Zhao, X.; Poon, Z.; Engler, A. C.; Bonner, D. K.; Hammond, P. T. *Biomacromolecules* **2012**, *13*, 1315−1322.
(37) Attia, A. B. E.; Ong, Z. Y.; Hedrick, J. L.; Lee, P. P.; Ee, P. L. R.; Hammond, P. T.; Yang, Y.-Y. *Curr. Opin. Colloid Interface Sci.* **2011**, *16*, 182−194.
(38) Shahin, M.; Lavasanifar, A. *Int. J. Pharm.* **2010**, *389*, 213−222.
(39) Shi, Y.; van Steenbergen, M. J.; Teunissen, E. A.; Novo, L.; Gradmann, S.; Baldus, M.; van Nostrum, C. F.; Hennink, W. E. *Biomacromolecules* **2013**, *14*, 1826−1837.
(40) Sun, Y.; Zou, W.; Bian, S.; Huang, Y.; Tan, Y.; Liang, J.; Fan, Y. *Biomaterials* **2013**, *30*, 6818−6828.
(41) Shi, M.; Wosnick, J. H.; Ho, K.; Keating, A.; Shoichet, M. S. *Angew. Chem., Int. Ed. Engl.* **2007**, *46*, 6126−6131.
(42) Sawant, R. R.; Torchilin, V. P. *Methods Mol. Biol.*; Grobmyer, S. R.; Moudgil, B. M., Eds.; Humana Press: Totowa, NJ, 2010; Vol. *624*, pp 131−149.
(43) Flanary, S.; Hoffman, A. S.; Stayton, P. S. *Bioconjugate Chem.* **2009**, *20*, 241−248.
(44) Elsabahy, M.; Dufresne, M. H.; Leroux, J. C. *Handbook of Materials for Nanomedicine*; Pan Stanford Publishing: Singapore, 2011.
(45) Donini, C.; Robinson, D. N.; Colombo, P.; Giordano, F.; Peppas, N. A. *Int. J. Pharm.* **2002**, *245*, 83−91.
(46) Otsuka, H.; Nagasaki, Y.; Kataoka, K. *Adv. Drug Delivery Rev.* **2012**, 1−18.
(47) Ding, H.-M.; Ma, Y.-Q. *Biomaterials* **2012**, *33*, 5798−5802.
(48) Prencipe, G.; Tabakman, S. M.; Welsher, K.; Liu, Z.; Goodwin, A. P.; Zhang, L.; Henry, J.; Dai, H. *J. Am. Chem. Soc.* **2009**, *131*, 4783−4787.
(49) Kim, S.; Shi, Y.; Kim, J. Y.; Park, K.; Cheng, J.-X. *Expert Opin. Drug Delivery* **2010**, *7*, 49−62.
(50) Singla, A. K.; Garg, A.; Aggarwal, D. *Int. J. Pharm.* **2002**, *235*, 179−192.
(51) Cegnar, M.; Kristl, J.; Kos, J. *Expert Opin. Biol. Ther.* **2005**, *5*, 1557−1569.
(52) González, R. B.; Huwyler, J.; Boess, F. *Biopharm. Drug Dispos.* **2004**, *25*, 37−49.
(53) Izutsu, K.; Yoshioka, S.; Kojima, S.; Randolph, T. W. *Pharm. Res.* **1996**, *13*, 1393−1400.

(54) De Jaeghere, F.; Allémann, E.; Leroux, J.-C.; Stevels, W.; Feijen, J.; Doelker, E.; Gurny, R. *Pharm. Res.* **1999**, *16*, 859−866.
(55) Li, J. T.; Caldwell, K. D.; Rapoport, N. *Langmuir* **1994**, *10*, 4475−4482.
(56) Santander-Ortega, M. J.; Jodar-Reyes, A. B.; Csaba, N.; Bastos-Gonzalez, D.; Ortega-Vinuesa, J. L. *J. Colloid Interface Sci.* **2006**, *302*, 522−529.
(57) Adams, M. L.; Kwon, G. S. *J. Biomater. Sci.—Polym. E* **2002**, *13*, 991−1006.
(58) Overbeek, J. *J. Colloid Interface Sci.* **1977**, *58*, 408−422.
(59) Owens, D. E., III; Peppas, N. A. *Int. J. Pharm.* **2006**, *307*, 93−102.
(60) Devine, D. V.; Wong, K.; Serrano, K.; Chonn, A.; Cullis, P. R. *Biochim. Biophys. Acta, Biomembr.* **1994**, *1191*, 43−51.
(61) Foged, C.; Brodin, B.; Frokjaer, S.; Sundblad, A. *Int. J. Pharm.* **2005**, *298*, 315−322.
(62) Dobrovolskaia, M. A.; Aggarwal, P.; Hall, J. B. *Mol. Pharmaceutics* **2008**, *5*, 487−495.
(63) Cho, H.-J.; Yoon, H. Y.; Koo, H.; Ko, S.-H.; Shim, J.-S.; Lee, J.-H.; Kim, K.; Kwon, I. C.; Kim, D.-D. *Biomaterials* **2011**, *32*, 7181−7190.
(64) Kumar, V.; Prud'homme, R. K. *J. Pharm. Sci.* **2008**, *97*, 4904−4914.
(65) Nakanishi, T.; Fukushima, S.; Okamoto, K.; Suzuki, M.; Matsumura, Y.; Yokoyama, M.; Okano, T.; Sakurai, Y.; Kataoka, K. *J. Controlled Release* **2001**, *74*, 295−302.
(66) Mikhail, A. S.; Allen, C. *Biomacromolecules* **2010**, *11*, 1273−1280.
(67) Patel, S. K.; Lavasanifar, A.; Choi, P. *Biomaterials* **2010**, *31*, 1780−1786.
(68) Chan, D. P. Y.; Deleavey, G. F.; Owen, S. C.; Damha, M. J.; Shoichet, M. S. *Biomaterials* **2013**, *34*, 8408−8415.
(69) Du, J.; O'Reilly, R. *Soft Matter* **2009**, *5*, 3544−3561.
(70) Li, Y.; He, H.; Jia, X.; Lu, W.-L.; Lou, J.; Wei, Y. *Biomaterials* **2012**, *33*, 3899−3908.
(71) Rodriguez, P. L.; Harada, T.; Christian, D. A.; Pantano, D. A.; Tsai, R. K.; Discher, D. E. *Science* **2013**, *339*, 971−975.
(72) Fang, R. H.; Hu, C.-M. J.; Zhang, L. *Expert Opin. Biol. Ther.* **2012**, *12*, 385−389.